

DOI: 10.1002/anie.200600259

Proteolytic Actuation of Nanoparticle Self-Assembly***Todd J. Harris, Geoffrey von Maltzahn, Austin M. Derfus, Erkki Ruoslahti, and Sangeeta N. Bhatia**

Nature has evolved elegant strategies to temporally and spatially control the initiation of protein activity, including the synthesis of subunits that self-assemble to form a functional unit and the synthesis of proteins with prodomains that require cleavage for activation. Nanomaterials that exploit bio-inspired self-assembling motifs have been used for sensitive detection of DNA,^[1,2] proteins,^[3,4] viruses,^[5] and pH changes^[6] in vitro. In general, these systems employ complementary chemistries that are constitutively exposed and lack elements of temporal control that could broaden their applicability. Herein, inspired by the biological motif of initiating assembly by enzymatic removal of inhibitors, we demonstrate with peptide-polymer chemistry that inorganic nanoparticles may be functionalized to exist in a “latent” state until triggered by a protease to self-assemble.

We inhibit the binding of biotin and neutravidin coated superparamagnetic Fe₃O₄ nanoparticles with polyethylene glycol (PEG) polymers that may be proteolytically removed to initiate assembly by matrix metalloproteinase-2 (MMP-2), a protease correlated with cancer invasion, angiogenesis, and metastasis.^[7–9] We demonstrate that MMP-2 initiated assembly amplifies the transverse (T2) relaxation of nanoparticle

[*] T. J. Harris,^[†] G. von Maltzahn,^[†] Prof. S. N. Bhatia
Harvard-MIT Division of Health Sciences and Technology
Massachusetts Institute of Technology
E19-502D Cambridge, MA 02139 (USA)
Fax: (+1) 617-324-0710
E-mail: sbhatia@mit.edu

Prof. S. N. Bhatia
Electrical Engineering and Computer Science/MIT
Brigham & Women's Hospital
Boston, MA (USA)

A. M. Derfus
Department of Bioengineering
University of California
San Diego, La Jolla, CA (USA)

E. Ruoslahti
Burnham Institute
La Jolla, CA (USA)

[†] These authors contributed equally

[**] This work was supported by NCI/NASA (N01-CO37117) and NCI (U54 CA119349 and U54 CA119335). T.J.H. acknowledges support from the NIH-NIBIB (EB 006324). G.v.M. acknowledges support from the Whitaker Foundation. We thank Dr. Daniel Sodickson and Dr. Aaron Grant for assistance with MRI, Dr. Deborah Burstein at the Beth Israel Deaconess Medical Center for the use of the 4.7T MRI, Yusuke Nagai for help with atomic force microscopy, and Dr. Michael Sailor for helpful discussions.

solutions in magnetic resonance imaging (MRI), enables magnetic manipulation with external fields, and allows MRI detection of tumor-derived cells that produce the protease. In the future, this general approach may enable site-selective immobilization and enhanced image contrast in regions of tumor invasion *in vivo*.

The synthesis of proteolytically actuated, self-assembling nanoparticles involves modifying them to be self-complementary but rendered latent by protease-cleavable elements (Figure 1). Briefly, 50 nm dextran-coated Fe₃O₄ nanoparticles,

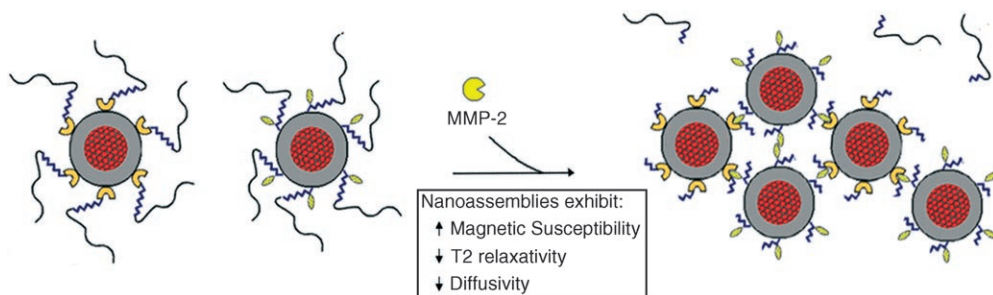


Figure 1. Schematic representation of a proteolytic actuation of self-assembly. Neutravidin- and biotin-functionalized superparamagnetic iron oxide nanoparticles are inhibited by the attachment of PEG chains that are anchored by MMP-2-cleavable peptide substrates (GPLGVRGC). Upon proteolytic removal of PEG through cleavage of the peptides, biotin and neutravidin particles self-assemble into nanoassemblies with enhanced magnetic susceptibility, T2 magnetic resonance relaxation, and lowered diffusivity.

sized by analytical ultracentrifugation (Micromod, Germany), were modified with either biotin or neutravidin (Pierce, Rockford, IL) to generate two populations of particles. When combined in solution, these particles self-assemble through highly stable biotin–neutravidin interactions. To allow enzymatic control of particle assembly, the nanoparticle surfaces of both populations are modified with the MMP-2 peptide substrate, GPLGVRGC,^[10] which serves as an anchor for linear PEG chains. PEG is a highly mobile, hydrophilic polymer with a large sphere of hydration that has been widely used to deter adsorption of proteins or cells on surfaces and to extend therapeutic circulation times *in vivo*.^[11,12] We hypothesized that linear PEGs of appropriate lengths would inhibit association of 50 nm nanoparticles but still allow MMP-2 proteases (< 9 nm^[13]) to cleave peptide linkers. To explore this idea, we conjugated PEGs of varying molecular weights (2, 5, 10, and 20 kDa) to biotin and neutravidin particles through MMP-2-cleavable linkers, and tested their ability to assemble with and without MMP-2. The rate and extent of assembly was measured by monitoring changes in the solution extinction at 600 nm (Figure 2a). Assembly of PEG-coated biotin and neutravidin particles without MMP-2 was found to be inversely related to PEG molecular weight with almost complete inhibition of particle assembly at lengths of 10 kDa or higher. Nanoparticles incubated with MMP-2 also aggregated at a rate inversely related to PEG chain length, likely owing to a similar steric repulsion of MMP-2. A comparison of the change in extinction of particles incubated with MMP-2 with those without MMP-2 incubation at 3 h showed that the 5 kDa and 10 kDa PEGs allow the highest MMP-2-catalyzed assembly

enhancement (Figure 2b). However, because the 5 kDa PEG cannot completely inhibit particle interaction in their latent state, the 10 kDa PEG was chosen as the optimum surface modification.

To further verify that the particle assembly was due to the sequence-specific release of PEG by MMP-2, a scrambled linker with low cleavage specificity by MMP-2, GPVGLRGC,^[14] was generated and conjugated to the particles. The nanoparticles with the scrambled peptide exhibit markedly decreased assembly compared with the specific peptide sequence (Figure 2c). At 3 h, following MMP-2 addition, assemblies of nanoparticles with specific MMP-2 substrates, examined by AFM, were as large as 0.5–1 μm. This suggests assembly of 10s to 100s of particles. The nanoparticles that are not incubated with MMP-2 remained dispersed with diameters of ≈ 75 nm (Figure 2d).

Nanoassemblies of iron oxide particles that form upon proteolytic activation acquire emergent magnetic properties that may be remotely detected with MRI. The coordination of superparamagnetic Fe₃O₄ magnetic dipoles in assembled nanoparticles amplifies the diffusional dephasing of surrounding water molecules and causes shortening of T2 relaxation times in MRI.^[15,16] We demonstrate that measurement of T2 changes allows sensitive, remote detection of protease-triggered assembly across a tenfold variation in particle concentration (Figure 3). The concentrations used correspond to 0.7–7 mg Fe/kg of solution, spanning the working concentrations typically utilized for tumor and lymphatic targeting *in vivo* (2.6 mg Fe/kg body weight).^[17]

Nanoparticle solutions were incubated with varying concentrations of MMP-2 in a 384-well plate, and their T2 relaxation times were mapped by using a Carr-Purcell-Meiboom-Gill (CPMG) sequence on a 4.7T Bruker MRI. T2 shifts of greater than 150 ms were observed by MMP-2-triggered assembly in a 3.2 μm nanoparticle solution. For 10 μm and 32 μm concentrations, a T2 shortening of approximately 50% of the starting value was observed after incubation with MMP-2. Nanoparticles at a 10 μm concentration were sensitive to at least 170 ng mL⁻¹ (9.4 U mL⁻¹) of MMP-2, which compares favorably with levels found in tumor tissue of MMP-2-expressing cancer cells (435 U/g MMP-2).^[14]

Next, the utility of the protease-triggered nanoparticles was explored in complex biological specimens in which nonspecific protein adsorption is often problematic. Specifically, latent nanoparticles were incubated in cell-culture medium above living human fibrosarcoma cells, HT-1080s, which constitutively express and activate MMP-2.^[18,19] MMP-2 is a zinc-binding protease with cleavage specificity for Type IV collagen, the principal constituent of basement membranes. Upregulation of MMP-2 activity leads to invasive proliferation and metastases of cancer cells by breaking down

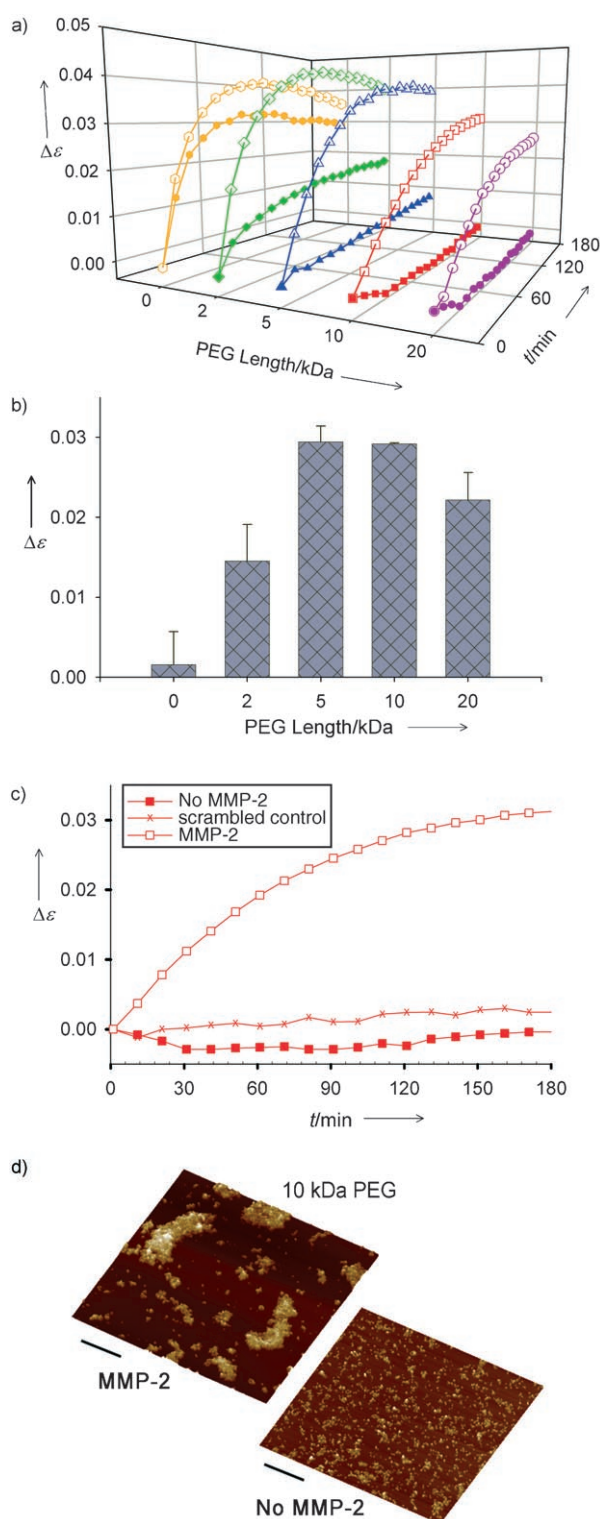


Figure 2. The role of PEG length and characterization of assembly. a) Changes in light scattering of nanoparticles over time with MMP-2 ($11 \mu\text{g mL}^{-1}$; hollow) or without MMP-2 (solid) shows the influence of PEG length on particle aggregation kinetics. b) The difference between extinction of particles with and without MMP-2 after 3 h reveals an optimal PEG chain length of 10 kDa. c) Nanoparticles with a specific MMP-2 substrate aggregate in the presence of MMP-2 ($11 \mu\text{g mL}^{-1}$), whereas particles with a scrambled peptide do not. d) Atomic force micrographs of particle solutions in (c) confirm aggregation of particles in the presence of MMP-2. Scale bars are 500 nm.

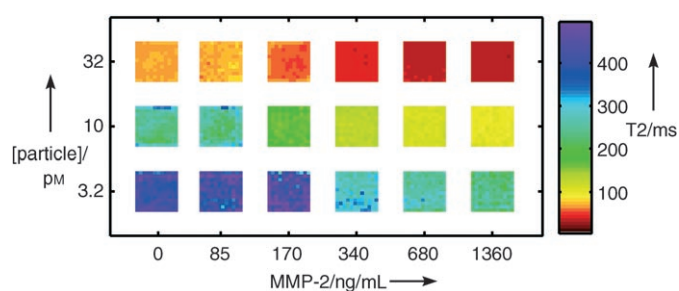


Figure 3. The triggered self-assembly of MMP-2 results in detectable changes in T2 relaxation times. T2 maps generated by a 4.7T Bruker MRI shows detectable aggregation after 3 h with the addition of 85, 170, 340, 680, and 1360 ng mL^{-1} MMP-2 for nanoparticle concentrations of 32 μM , 10 μM , and 3.2 μM .

tissue barriers.^[7,8] Nanoparticles (10 μM) were incubated over HT-1080 cells for 5 h, and T2 maps of media samples were generated with MRI. A substantial shortening in T2 was detected in the media over HT-1080 cells compared with media over cells incubated with the broad-spectrum MMP inhibitor Galardin (Figure 4a).

Triggered assembly of the nanoparticles can also be used to magnetically target nanoassemblies to cells. As the magnetic domains of coalesced nanoparticles coordinate to form an amplified cumulative dipole, they become more susceptible to long-range dipolar forces.^[20] This phenomenon, similar to the T2 relaxivity enhancement in MRI, allows manipulation of the nanoassemblies with imposed magnetic fields, whereas isolated particles remain unaffected. By using a high-gradient permanent magnet, MMP-2 triggered assemblies of iron oxide particles (1.5 nm) can be visually drawn out of solution, whereas nonactivated particles remain dispersed (Figure 4b). To demonstrate that this can be extended towards targeting particles onto cancer cells, HT-1080 cultures were placed over a strong permanent magnet and incubated with nanoparticles at a 150 μM concentration. After 3 h, the media was removed and the cells were washed, fixed, and stained for aggregates by using a biotinylated fluorescent probe. Bright fluorescent staining of particle assemblies is seen over HT-1080 cells, whereas weak diffuse staining, indicating little to no targeting, is seen over cells incubated with the inhibitor Galardin (Figure 4c).

To the best of our knowledge, this report represents the first demonstration of protease-triggered nanoparticle self-assembly. This system differs from the reported use of enzymatic cleavage to prevent assembly,^[2,21,22] rather it exploits proteolytic activity to construct multimeric assemblies with emergent properties. Previously, our laboratories have demonstrated that peptide-modified semiconductor quantum dots could precisely target tumors in whole animals^[23] and subcellular organelles in living cells.^[24] This report extends the ability of nanoparticles not only to target sites of interest, but to interact with the processes of disease by harnessing biological machinery to assemble nanomaterials with amplified properties. We show that polymeric protection can temporarily shield dissimilar complementary ligands, including both small molecules (biotin) and tetrameric proteins (neutravidin). Accordingly, in contrast to recent

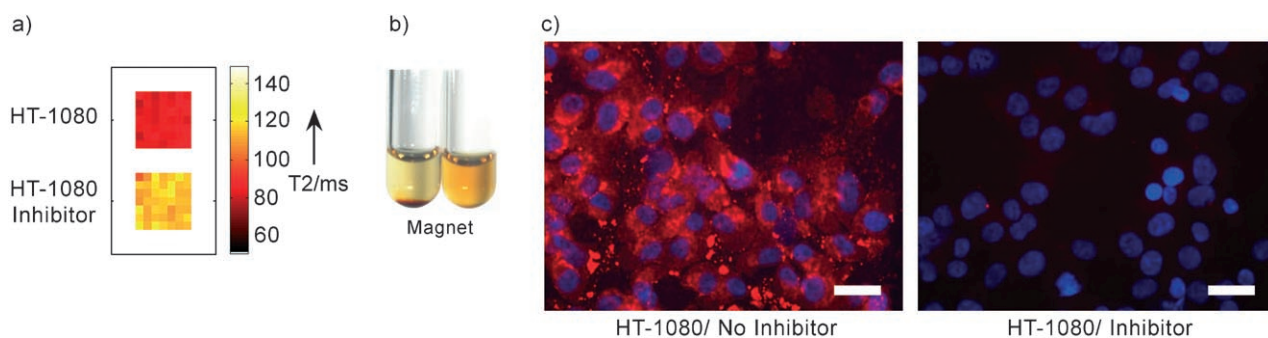


Figure 4. Triggered self-assembly of nanoparticles by HT-1080 Tumor-derived cells. a) T2 mapping of Fe_3O_4 nanoparticles incubated for 5 h over HT-1080 cells that secrete active MMP-2 in a complex medium. Nanoparticle assembly amplifies T2 relaxation over cancer cells relative to cells incubated with the MMP inhibitor Galardin at $25 \mu\text{M}$. b) Activated nanoparticles are drawn out of solution by a strong magnet (left) whereas inactive nanoparticles (right) are not. c) Nanoparticles activated by MMP-2-secreting tumor cells for 3 h are drawn out of solution onto cells by a magnetic field. Available neutravidins on aggregates are stained with biotin-quantum dots (emission: 605 nm) and imaged by epifluorescent microscopy. Assemblies are not targeted to cells if an MMP inhibitor is used. Scale bar represents $50 \mu\text{m}$.

reports of proteolytic activation of cell-penetrating peptides^[19] and peroxidase-initiated nanoparticle assembly,^[4,25] our approach can be considered entirely modular and thereby generalizable. Therefore, key features, for example, biochemical triggers and molecular recognition, may be altered without significant re-engineering. Formulations with new functionalities could be easily developed by substituting the complementary binding pairs, cleavable substrates (e.g. glycans, lipids, oligonucleotides), or multivalent nanoparticle cores (e.g. gold, quantum dot, dendrimer) to extend the capabilities of existing modalities.

Experimental Section

Synthesis of nanoparticle probes: Protease-triggered, self-assembling nanoparticles were synthesized by using amine-functionalized, dextran-coated iron-oxide nanoparticles (50 nm ; 6.25 pmol/mg Fe), sized by analytical ultracentrifugation (Micromod (Germany)). All peptides were obtained at $>90\%$ purity (Synpep), and all reagents were obtained from Sigma unless otherwise specified. A high-gradient magnetic-field filtration column was used between each conjugation (Miltenyi Biotec) and all conjugations were performed at room temperature unless stated. Peptides were synthesized to sequentially contain a lysine (for the attachment of polyethylene glycol polymers), an MMP-2 cleavage sequence (or scrambled version), and a terminal cysteine (for linkage onto amines in the dextran coat or lysines on neutravidin proteins). Phosphate-buffered saline buffer solution (PBS; Na_2PO_4 (0.1 M), NaCl buffer (0.15 M)). For biotin probes, *N*-Succinimidyl-3-[2-pyridyldithio]-propionamide (SPDP; 0.25 mg mL^{-1}) was treated with particle amines (2.5 mg Fe ; PBS (1 mL), $\text{pH } 7.2$; 1 hr), after which cysteine-containing peptides (acetyl-KGPLGVGRC-X-Biotin (1 mg mL^{-1})) were added to displace pyridine-2-thione leaving groups (PBS (1 mL) with EDTA (10 mM), $\text{pH } 7.2$; 12 h under N_2 ; 4°C). Polyethylene glycol polymers with a terminal methoxy cap at one end and an opposing amine-reactive succinidyl α -methylbutanoate (mPEG-SMB) (Nektar; 2.5 mM) were then attached to peptide lysines (PBS (1 mL), $\text{pH } 7.2$; 3 h). Neutravidin (Pierce) nanoparticles were formed by modifying particles (2.5 mg Fe) with biotinamidohexanoyl-6-amino-hexanoic acid *N*-hydroxy-succinimide ester (0.5 mg mL^{-1} ; PBS (1 mL); $\text{pH } 7.2$; 1 h) and then coated with a saturating concentration of neutravidin ($850 \mu\text{g}$ neutravidin per 2.5 mg nanoparticles; PBS (5 mL), $\text{pH } 7.2$; $>3 \text{ h}$). The extinction of the solution at 600 nm was measured during incubation to ensure no aggregate formation. Additionally, neutravidin-coated particles were passed through a $0.1 \mu\text{m}$ filter to confirm

monodispersity. By using the same conditions described for biotin particle conjugations, peptides (KGPLGVGRC) were linked to available lysine amines on neutravidin-coated nanoparticles with SPDP, after which mPEG-SMB polymers were linked to peptide lysines. Scrambled sequences used for control experiments contained GVRLGPG instead of GPLGVGRC. Extinction, AFM, and magnetic field migration measurements: For all assembly experiments, equimolar ratios of particles were used. All extinction measurements were performed in duplicate in 384-well plates by using a SpectraMax Plus spectrophotometer (Molecular Devices, Sunnyvale CA). Biotin and neutravidin probes (0.5 mg mL^{-1} ; 2-[4-(2-hydroxyethyl)-1-piperazinyl]ethanesulfonic acid (HEPES; 0.1 M), CaCl_2 (5 mM); $\text{pH } 7.2$) were mixed at equal ratios and $0.5 \mu\text{g}$ of the recombinant catalytic domain of MMP-2 (Biomol.) ($6 \mu\text{L}$ Tris-Cl (50 mM), CaCl_2 (5 mM), Brij-35 (0.005%); $\text{pH } 7.5$) was added to $40 \mu\text{L}$ probe solution at time zero. For controls, $6 \mu\text{L}$ of buffer without MMP-2 was added. The same probe and MMP-2 concentrations were used for AFM and solution phase magnetic precipitation experiments. AFM measurements were performed by using a multimode, Digital Instruments AFM (Santa Barbara CA) operating in tapping-mode by using FESP Tips (Veeco Nanoprobe TM, Santa Barbara CA). AFM reactions were incubated for 3 h , diluted, and evaporated on freshly cleaved mica for analysis. In magnetic precipitation experiments, probe solutions were incubated with or without MMP-2 overnight and placed over a strong magnet for 2.5 min .

MRI detection of self-assembly: MRI images were taken on a Bruker 4.7T magnet, 7 cm bore. Biotin-peptide-P-EG and neutravidin-peptide-PEG nanoparticles were mixed together and serially diluted in 384-well plate. Serial dilutions of recombinant MMP-2 in $6 \mu\text{L}$ of buffer solution (Tris-Cl (50 mM), CaCl_2 (5 mM), Brij-35 (0.005%); $\text{pH } 7.5$) were added to each well. After 3 h , a CPMG sequence of 16 images with multiples of 10.45 ms echo times and a relaxation time of 5000 ms were acquired. T2 maps were obtained for each well by fitting images on a pixel by pixel basis to the equation $y = M^* \times 10^{(-TE/T2)}$ by using MATLAB.

Cell culture: HT-1080 human fibrosarcoma cells (ATCC) were cultured in 24-well plates by using minimum essential medium eagle (Invitrogen) with fetal bovine serum (10% ; Invitrogen) and penicillin/streptomycin (1%). For MRI experiments, the media was replaced with serum-free dubelcco's modified eagle medium (DMEM; Invitrogen) with a 10 pM nanoparticle concentration. The broad-spectrum MMP-2 inhibitor Galardin (Biomol) was added at a concentration of $25 \mu\text{M}$ in control cultures. Samples of $40 \mu\text{L}$ were taken at 5 h for MRI imaging by using the same procedures for T2 mapping described above. For fluorescent labeling experiments, media was replaced with serum-free DMEM with a 200 pM nanoparticle concentration and cells were placed over a strong magnet.

After 3 h, the media was removed and the cells fixed with paraformaldehyde (2%). The cells were permeabilized with Triton-X (0.1%) in PBS and incubated with biotin quantum dots (emission = 605 nm; Quantum Dot Corp). Nuclear staining was performed by incubating with Hoescht (0.001%) for 1 min.

Received: January 20, 2006

Revised: March 11, 2006

Keywords: magnetic properties · nanostructures · proteases · self-assembly · triggered assembly

-
- [1] C. A. Mirkin, R. L. Letsinger, R. C. Mucic, J. J. Storhoff, *Nature* **1996**, 382, 607.
- [2] J. M. Perez, L. Josephson, T. O'Loughlin, D. Hogemann, R. Weissleder, *Nat. Biotechnol.* **2002**, 20, 816.
- [3] D. G. Georganopoulou, L. Chang, J. M. Nam, C. S. Thaxton, E. J. Mufson, W. L. Klein, C. A. Mirkin, *Proc. Natl. Acad. Sci. USA* **2005**, 102, 2273.
- [4] J. M. Perez, F. J. Simeone, A. Tsourkas, L. Josephson, R. Weissleder, *Nano Lett.* **2004**, 4, 119.
- [5] J. M. Perez, F. J. Simeone, Y. Saeki, L. Josephson, R. Weissleder, *J. Am. Chem. Soc.* **2003**, 125, 10192.
- [6] M. M. Stevens, N. T. Flynn, C. Wang, D. A. Tirrell, R. Langer, *Adv. Mater.* **2004**, 16, 915.
- [7] G. Giannelli, J. FalkMarzillier, O. Schiraldi, W. G. StetlerStevenson, V. Quaranta, *Science* **1997**, 277, 225.
- [8] D. R. Edwards, G. Murphy, *Nature* **1998**, 394, 527.
- [9] J. M. Fang, Y. Shing, D. Wiederschain, L. Yan, C. Butterfield, G. Jackson, J. Harper, G. Tamvakopoulos, M. A. Moses, *Proc. Natl. Acad. Sci. USA* **2000**, 97, 3884.
- [10] J. L. Seltzer, K. T. Akers, H. Weingarten, G. A. Grant, D. W. Mccourt, A. Z. Eisen, *J. Biol. Chem.* **1990**, 265, 20409.
- [11] J. M. Harris, R. B. Chess, *Nat. Rev. Drug Discovery* **2003**, 2, 214.
- [12] R. Gref, Y. Minamitake, M. T. Peracchia, V. Trubetskoy, V. Torchilin, R. Langer, *Science* **1994**, 263, 1600.
- [13] E. Morgunova, A. Tuuttila, U. Bergmann, M. Isupov, Y. Lindqvist, G. Schneider, K. Tryggvason, *Science* **1999**, 284, 1667.
- [14] C. Bremer, C. H. Tung, R. Weissleder, *Nat. Med.* **2001**, 7, 743.
- [15] R. A. Brooks, F. Moiny, P. Gillis, *Magn. Reson. Med.* **2001**, 45, 1014.
- [16] P. Gillis, F. Moiny, R. A. Brooks, *Magn. Reson. Med.* **2002**, 47, 257.
- [17] M. G. Harisinghani, J. Barentsz, P. F. Hahn, W. M. Deserno, S. Tabatabaei, C. H. van de Kaa, J. de la Rosette, R. Weissleder, *N. Engl. J. Med.* **2003**, 348, 2491.
- [18] C. Bremer, S. Bredow, U. Mahmood, R. Weissleder, C. H. Tung, *Radiology* **2001**, 221, 523.
- [19] T. Jiang, E. S. Olson, Q. T. Nguyen, M. Roy, P. A. Jennings, R. Y. Tsien, *Proc. Natl. Acad. Sci. USA* **2004**, 101, 17867.
- [20] Y. Lalatonne, J. Richardi, M. P. Pileni, *Nat. Mater.* **2004**, 3, 121.
- [21] M. Zhao, L. Josephson, Y. Tang, R. Weissleder, *Angew. Chem.* **2003**, 115, 1413; *Angew. Chem. Int. Ed.* **2003**, 42, 1375.
- [22] J. M. Perez, T. O'Loughlin, F. J. Simeone, R. Weissleder, L. Josephson, *J. Am. Chem. Soc.* **2002**, 124, 2856.
- [23] M. E. Akerman, W. C. W. Chan, P. Laakkonen, S. N. Bhatia, E. Ruoslahti, *Proc. Natl. Acad. Sci. USA* **2002**, 99, 12617.
- [24] A. M. Derfus, W. C. W. Chan, S. N. Bhatia, *Adv. Mater.* **2004**, 16, 961.
- [25] A. Bogdanov, Jr., L. Matuszewski, C. Bremer, A. Petrovsky, R. Weissleder, *Mol. Imaging* **2002**, 1, 16.
-